THE ASTROPHYSICAL JOURNAL, 316:449–457, 1987 May 1

INTERDEPENDENCE OF THE 4430 Å DIFFUSE INTERSTELLAR BAND, POLARIZATION, AND ULTRAVIOLET EXTINCTION

J. KREŁOWSKI,[1,2] G. A. H. WALKER, G. R. GRIEVE, AND G. M. HILL[2]
Geophysics and Astronomy Department, University of British Columbia
Received 1986 July 1; accepted 1986 October 13

ABSTRACT

We present central intensities of the 4430 Å diffuse interstellar band (DIB) measured from Reticon spectra for 128 early type stars. Stars in the Perseus OB1 association have significantly higher ratios of polarization and $E(15-18)$ color excess to $E(B-V)$ and significantly weaker 4430 Å than do the stars in Cepheus OB3. The ratio of the color excess $E(22-33)$ to $E(B-V)$ is marginally low in Cepheus OB3. There is a significant correlation between the A_{4430} anomaly and $E(15-18)$. While the unusual correlations for Per OB1 could have independent causes, it is suggested that the $\lambda 4430$ absorption and far-UV extinction in fact depend on grain orientation. It is further suggested that the $\lambda 4430$ absorption arises in a thin grain mantle and the 2200 Å feature in the grain core. The absence of 4430 Å DIB in high Galactic latitude clouds would be due to a l{ack of a mantle. The DIB ratio $\lambda 5780/\lambda 5797$ closely mimics the behavior of the ratio $\lambda 4430/E(B-V)$ for seven stars from a range of Galactic latitudes which confirms the existence of the three families of DIBs identified in an earlier paper.

Subject headings: interstellar: matter — polarization — ultraviolet: spectra

I. INTRODUCTION

The 4430 Å diffuse interstellar band (DIB) was discovered and announced as interstellar 50 years ago by Merrill (1936). Being strong and occurring near the peak sensitivity of blue photographic plates, it has probably attracted more attention than the other DIBs. Duke (1951) made the first extensive survey of its strength from photographic spectra and demonstrated that it is at least 40 Å in width. Duke showed that the band strength can be more accurately estimated from the central depth, because measurements of the equivalent width are more sensitive to errors in the placing of the continuum.

Subsequently, the feature was measured photoelectrically by a number of authors (Baerentzen *et al.* 1967; Walker 1963; Wampler 1966). The profile of the 4430 Å DIB is hard to measure, particularly in the wings, and estimates of the full width vary from 150 Å (Wilson 1958) to the more generally accepted value of 40 Å (Seddon 1967). As with other DIBs, the origin is still unknown.

With modern solid-state detectors it is possible to define the behavior of the DIBs better, particularly for stars of small color excess where the line of sight may intersect only one or two interstellar clouds. In this paper we draw attention to an effect which may directly relate both the far-UV extinction by interstellar grains and the source of the 4430 Å absorption to the grain orientation. The effect is probably related to the existence of three families among the DIBs, which we discuss in another paper (Krełowski and Walker 1987). For stars at high Galactic latitude: (1) the 4430 and 6180 Å DIBs are absent; (2) the 5780, 6196, 6203, 6279, and 6284 Å DIBs are about one-third of expected strength; and (3) the 2200 Å feature and the 5797, 5850, 6376, 6379, and 6614 Å DIBs are of approximately normal strength.

[1] On leave from N. Copernicus University, Toruń, Poland.
[2] Guest Observer at Dominion Astrophysical Observatory, Victoria, which is operated by the Herzberg Institute of Astrophysics.

II. OBSERVATIONS

All the spectra were obtained with refrigerated E.G. and G. RL 1872F/30 Reticon detectors built in our department (Walker, Johnson, and Yang 1985), using the spectographs on the UBC 0.4 m, DAO 1.22 m, or 1.8 m telescopes at 76, 40, or 60 Å mm^{-1}, respectively. The corresponding sampling by the 15 μm diodes corresponds to 1.14, 0.6, 0.9 Å per diode. The data acquisition, calibration, and reduction has been fully described by Walker *et al.*

The 128 program stars are listed in Table 1. Most are supergiants and slightly reddened dwarfs observed for other programs, and they range in spectral type from O to early A. Successive columns give: HD number, spectral type and luminosity class, galactic longitude and latitude, $E(B-V)$; the color excesses $E(22-33)$ and $E(15-18)$ where available based on observations with the *ANS* (Wesselius *et al.* 1982) and intrinsic colors from Galecki *et al.* (1983), polarization in magnitudes from Hiltner (1956) for the stars in the Perseus OB1 and Cepheus OB3 associations only, our measurements of the central depths of the 4430 Å DIB as a percentage of the continuum, and indications of the telescope and dispersion used and association membership.

The wavelength calibration of the spectra and normalization to a continuum has been described by Krełowski and Walker (1987). Figure 1 shows four spectra of stars with different color excesses and also indicates the points chosen for the continuum. (HD 91316, used as an unreddened standard, does not appear in Table 1.) The average signal-to-noise ratio per diode in all the measured spectra was ~ 700. Some of the prominent stellar absorption features are indicated. The spectrum of HD 190603 also shows the 4358 Å emission line from the mercury vapor street lamp outside the UBC dome. In measuring the central depths, profiles were drawn in by hand, with allowance being made for the obvious stellar absorption lines, which change with spectral type and luminosity class.

There are 17 stars for which A_{4430} was measured on two spectra (indicated by more than one of "A," "B," or "C" in the

TABLE 1

$A_c(\lambda4430)$ MEASUREMENTS

HD Number	Sp.Type	l	b	E(B-V)	E(22-33)	E(15-18)	p	A_c(4430)	Remarks
2905......	B1Iae	120.8	0.1	0.31	1.70	0.11	0.032	5.2	A,C,a
8065......	A0Iab	124.6	16.0	0.38	...	...	...	2.5	C
12953......	A1Iae	132.9	−2.9	0.59	3.15	0.52	0.074	4.6	B,C,b
13267......	B5Ia	133.5	−3.6	0.41	2.02	0.18	0.088	4.2	B,C,b
13402......	B0.5Ia	133.1	−1.7	0.81	...	...	0.116	8.6	B,b
13476......	A3Iab	133.5	−2.6	0.54	...	...	0.090	6.2	B,C,b
13659......	B1Ib	134.2	−4.1	0.70	3.06	0.61	0.080	5.0	B,b
13744......	A0Iab	133.9	−2.8	0.73	3.88	0.51	0.092	7.5	B,b
13745......	B0III	134.6	−5.0	0.43	2.28	0.23	0.063	4.2	A,b
13841......	B2Ib	134.4	−3.9	0.39	...	...	0.073	5.3	B,b
13854......	B1Ia	134.4	−3.9	0.45	...	...	0.083	5.1	B,b
13866......	B2Ib	134.5	−4.2	0.35	...	...	0.073	4.6	B,b
14052......	B1Ib	134.5	−3.7	0.47	...	...	0.088	4.8	B,b
14134......	B3Ib	134.6	−3.7	0.60	2.74	0.16	0.084	4.9	B,b
14143......	B2Ia	134.6	−3.7	0.66	...	...	0.086	6.1	B,b
14322......	B8Ia	135.3	−4.8	0.36	1.84	0.36	0.066	4.4	B,b
14433......	A1Ia	135.0	−3.5	0.55	3.30	0.43	0.086	4.7	B,b
14443......	B2Ia	135.0	−3.6	0.50	...	...	0.082	5.4	B,b
14489......	A2Ia	135.5	−4.8	0.32	...	...	0.049	4.2	B,C,b
14535......	A2Ia	135.1	−3.4	0.66	...	...	0.077	5.9	B,b
14542......	B8Ia	135.1	−3.3	0.64	3.34	0.31	0.067	6.5	B,b
14818......	B2Ia	135.6	−3.9	0.47	2.79	0.20	0.081	6.0	B,b
14899......	B8Ib	135.5	−3.3	0.47	2.59	0.34	0.070	5.5	B,b
14956......	B2Ia	135.4	−2.9	0.88	4.58	0.55	0.078	8.0	B,b
15497......	B6Ia	136.0	−2.6	0.84	4.26	0.50	0.096	7.1	B,b
15620......	B8Iab	136.1	−2.3	0.88	4.36	...	0.111	9.3	B,b
15690......	B1.5Ib	136.3	−2.7	0.82	4.29	0.54	0.115	6.6	B,b
16778......	A2Ia	136.6	−0.0	0.85	...	...	0.114	6.7	B,b
16779......	B2Ib	137.4	−1.8	0.90	5.42	0.44	0.102	7.7	B,b
17088......	B9Ia	137.9	−1.7	0.82	4.10	0.40	0.085	8.2	B,b
17145......	B8Ia	138.0	−1.8	0.86	4.52	0.43	0.096	9.1	B,b
17378......	A5Ia	138.5	−2.2	0.79	...	...	0.101	7.1	B,b
BD+60°493	B0.5Ia	134.6	0.6	0.99	...	...	0.091	8.2	B,b
18537......	B7V	142.1	−5.6	0.07	...	...	...	1.8	B,c
20041......	A0Ia	141.6	−0.4	0.71	4.12	0.25	...	7.3	B,d
20365......	B3IV	145.6	−6.1	0.14	0.84	−0.05	...	1.9	B,c
20418......	B5V	145.7	−6.1	0.10	0.61	−0.01	...	1.4	B,c
20809......	B5V	146.8	−6.5	0.09	0.51	−0.01	...	2.2	B,c
20863......	B8.5V	147.6	−6.5	0.09	0.28	−0.10	...	1.4	B,c
21071......	B7V	147.2	−6.3	0.05	0.22	−0.06	...	1.6	B,c
21181......	B8.5V	148.3	−6.5	0.09	0.41	−0.02	...	1.1	B,c
21278......	B5V	147.5	−6.2	0.07	...	...	...	1.6	B,c
21291......	B9Ia	141.5	2.9	0.41	2.30	0.18	0.075	3.5	C,d
21362......	B6Vn	147.2	−5.5	0.08	0.57	−0.02	...	1.4	B,c
21389......	A0Iae	142.2	2.1	0.54	3.17	0.10	0.075	5.3	B,d
21428......	B3V	147.5	−5.7	0.11	0.61	0.00	...	1.4	B,c
21455......	B7V	148.9	−7.8	0.25	1.01	0.13	...	1.6	B,c
21551......	B8V	148.4	−6.7	0.07	0.35	−0.03	...	1.4	B,c
21641......	B8.5V	149.1	−6.4	0.08	0.29	−0.07	...	1.6	B,c
21672......	B8V	148.6	−5.6	0.09	0.35	−0.04	...	1.7	B,c
22136......	B8IV	150.1	−6.5	0.10	0.38	−0.08	...	1.2	B,c
22928......	B5III	150.3	−5.8	0.03	0.11	−0.03	...	0.7	B,c
23302......	B6IIIe	166.2	−23.9	0.05	0.08	−0.07	...	1.2	B,e
23432......	B8V	166.1	−23.4	0.07	...	...	...	2.3	B,e
23850......	B8III	167.0	−23.2	0.02	0.06	−0.02	...	1.2	B,e
23923......	B8V	167.4	−23.4	0.06	0.32	0.03	...	1.6	B,e
24398......	B1Ib	162.3	−16.7	0.29	...	...	...	0.5	A,C,f
24504......	B6V	151.9	−4.3	0.04	...	...	...	0.9	B,c
24534......	O9.5ep	163.1	−17.1	0.59	...	...	0.025	7.9	A,f
24760......	B0.5V	157.4	−10.1	0.08	...	0.05	...	1.9	A,f
25940......	B3V	153.7	−3.0	0.17	1.05	−0.01	...	2.6	B,c
30614......	O9.5Iae	157.4	−10.1	0.29	1.52	0.20	...	2.1	A,C,g
35600......	B9Ib	176.8	−2.7	0.16	...	...	...	2.3	C,h
36371......	B5Iab	168.1	−4.4	0.42	2.12	0.02	...	4.8	C,h
37022......	O6	209.0	−19.4	0.35	0.92	−0.14	...	2.4	B,i
37043......	O9III	209.5	−19.6	0.06	...	...	...	1.3	A,i
37055......	B3IV	207.0	−18.3	0.08	0.39	0.00	...	0.9	B,i
40111......	B0.5II	184.0	0.8	0.16	0.92	0.09	0.023	2.7	A,j
46056......	O8	206.3	−2.3	0.49	...	...	0.025	4.3	B,k
46106......	B1V	206.2	−2.1	0.39	...	...	...	5.3	B,k

TABLE 1—*Continued*

HD Number	Sp.Type	l	b	E(B-V)	E(22-33)	E(15-18)	p	A_c(4430)	Remarks
46149......	O9V	206.2	−2.0	0.47	...	...	0.000	5.2	B,k
46150......	O6	206.3	−2.1	0.46	2.32	0.11	0.016	5.9	B,k
46202......	O9V	206.3	−2.0	0.49	2.19	0.21	...	4.5	B,k
46223......	O5	206.5	−2.0	0.55	...	...	0.030	6.1	B,k
47382......	B0III	207.4	−0.8	0.42	...	...	0.017	5.6	B,k
47432......	O9.5Ib	210.0	2.1	0.44	2.01	0.21	...	3.3	A,l
47839......	O7Ve	202.9	2.2	0.08	0.39	0.00	...	0.8	A,l
87901......	B7V	226.4	48.9	0.02	...	0.03	...	0.8	B
164353......	B5Ib	29.7	12.6	0.10	0.64	−0.05	...	2.2	C,m
166937......	B8Iape	10.0	−1.6	0.26	1.19	−0.04	...	5.4	C,n
167264......	B0Ia	10.5	−1.8	0.32	1.36	0.00	0.000	4.5	A,o
185507......	B3V	43.3	−8.1	0.23	1.36	−0.02	...	2.5	B
187982......	A1Ia	61.9	−1.0	0.68	3.89	0.03	...	7.7	C,p
188001......	O8f	56.5	−4.3	0.34	1.50	0.18	...	3.0	A
188209......	O9.5Ib	81.0	10.1	0.21	0.95	0.15	...	2.2	A,C
190603......	B1.5Ia	69.5	0.4	0.70	3.58	0.23	0.018	7.3	C,q
190918......	B1Ib	72.6	2.1	0.40	...	...	...	5.0	B,r
226868......	B0Ib	71.3	3.1	1.09	4.59	0.41	0.108	5.8	A,r
191243......	B5Ib	71.7	1.0	0.24	...	...	...	3.6	C,r
193322......	O9V	78.1	2.8	0.42	2.00	0.06	...	3.6	A
194280......	B0Ib	77.2	0.9	1.01	4.96	0.29	0.094	5.3	A,s
195592......	O9.5Ia	82.7	2.8	1.12	...	...	0.027	8.0	A
195965......	B0V	85.7	5.0	0.24	1.39	0.03	0.020	3.0	B,t
198475......	B3Iae	85.8	1.5	0.53	2.66	0.07	0.061	6.6	B,C,t
198846......	B0V	77.7	−6.4	0.26	1.22	0.03	...	3.5	B
199216......	B1II	88.9	3.0	0.65	3.73	0.17	0.040	4.6	A,B,t
199478......	B8Iae	87.5	1.4	0.50	2.45	0.17	0.040	5.4	C,u
199579......	O6Ve	85.7	−0.3	0.38	1.64	0.14	0.020	1.9	A,B,t
202850......	B9Iab	84.2	−6.9	0.12	0.84	0.15	...	2.8	C,v
203064......	B0.5IV	87.6	−3.9	0.29	1.29	0.03	...	2.8	A,B,t
203938......	B0.5IV	90.6	−2.2	0.72	3.57	0.09	0.030	6.8	B,t
204172......	B0Ib	83.4	−10.0	0.17	0.82	0.16	...	2.3	A,C,v
206165......	B2Ib	102.3	7.2	0.46	2.56	0.27	...	4.6	C,w
206267......	O6f	99.3	3.7	0.54	2.60	0.12	...	4.1	A,B,w
207198......	O9IIe	103.1	7.0	0.59	2.75	0.37	...	3.7	A,C,w
207260......	A2Iae	102.3	5.9	0.47	2.85	0.51	0.037	5.3	C,w
208501......	B8Ib	100.4	1.7	0.76	3.05	0.47	0.035	4.6	C,w
209481......	O9V	102.0	2.2	0.38	1.77	0.12	...	2.9	A,w
209975......	O9Ib	104.9	5.4	0.36	1.71	0.15	0.023	4.0	A,C,w
210839......	O6If	103.8	2.6	0.58	2.84	0.11	0.024	4.2	A,w
212593......	B9Iab	99.9	−6.7	0.09	0.68	0.11	...	1.9	C
213087......	B0.5Ibe	108.5	6.4	0.60	2.86	0.24	0.017	6.5	C,x
214680......	O9V	96.7	−17.0	0.11	0.50	−0.01	...	0.9	A,y
216014......	B0.5V	110.7	5.4	0.56	2.99	0.08	0.035	8.2	B
216532......	O8V	110.0	2.8	0.87	4.25	−0.04	0.044	11.0	B,z
216898......	O8.5V	110.2	2.5	0.86	4.09	−0.04	0.085	12.9	B,z
217035......	B0V	110.6	3.0	0.75	3.62	−0.16	0.037	10.8	B,z
217086......	O6	110.2	2.7	0.96	4.45	−0.05	0.024	9.6	A,B,z
217297......	B1V	111.1	3.7	0.57	2.87	0.03	...	7.2	B,z
217312......	B0.5IV	110.6	2.9	0.65	3.27	−0.01	0.028	7.6	B,z
218066......	B1V	111.6	3.1	0.85	3.12	0.06	0.015	9.4	B,z
218323......	B0.5II	111.8	3.7	0.84	3.71	0.12	0.041	9.9	B,z
218342......	B0IV	111.7	2.9	0.70	3.17	0.17	0.041	9.3	B,z
218537......	B3V	111.7	3.0	0.18	0.99	−0.02	...	2.5	B
218915......	O9.5Iab	108.5	−6.8	0.30	1.41	0.22	0.025	2.5	A
223385......	A3Iae	115.9	1.2	0.61	...	...	0.026	7.2	C,aa
225094......	B3Iae	117.6	1.3	0.45	2.22	0.05	0.050	5.5	C,aa
225146......	B0Ib	117.2	−1.2	0.62	3.05	0.25	0.068	7.5	C,aa

REMARKS.—(A) DAO 1.22m coudé; 40 Å mm^{-1}. (B) DAO 1.83m Cassegrain; 60 Å mm^{-1}. (C) UBC 0.42m coudé; 76 Å mm^{-1}. (a) Cas OB14. (b) Per OB1. (c) α Per. (d) Cam OB1. (e) Pleiades. (f) Per OB2. (g) NGC 1502. (h) Aur OB1. (i) Ori OB1. (j) Gem OB1. (k) Mon OB2. (l) Mon OB1. (m) Coll 359. (n) Sgr OB1. (o) Sgr OB7. (p) Vul OB4. (q) Cyg R1. (r) Cyg OB3. (s) Cyg OB1. (t) Cyg OB7. (u) NGC 6991. (v) Cyg OB4. (w) Cep OB2. (x) Cep OB1. (y) Lac OB1. (z) Cep OB3. (aa) Cas OB5.

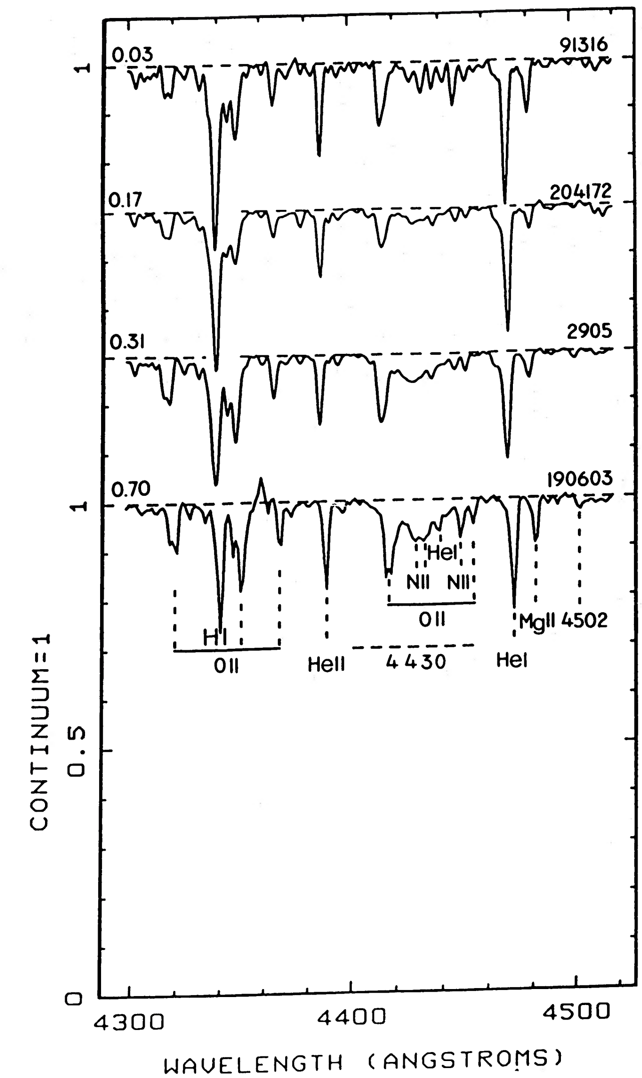

FIG. 1.—Reticon spectra in the region of the 4430 Å DIB for four stars with different amounts of interstellar reddening (indicated to the left of each spectrum). Some of the stronger stellar lines are identified. The spectra have been rectified to the continuum shown. The emission line at 4358 Å in the fourth spectrum is the night sky mercury line. HD numbers are given to the right of each spectrum.

Remarks col. of Table 1). From these multiple measurements we derive an rms error in a single determination of A_{4430} to be 0.4% of the continuum. Where there was more than one measurement of A_{4430} for a star, an average is given in Table 1.

III. DISCUSSION

The distribution of the stars in Table 1 is very nonuniform on the sky, with the majority being concentrated in associations. One-third are members of Perseus OB1 or Cepheus OB3. The stars from these two associations display significantly different correlations of the various measured quantities in Table 1 with $E(B-V)$. This is illustrated in Figures 2–5, in which A_{4430}, $E(22-33)$, $E(15-18)$, and p are plotted, respectively, against $E(B-V)$ (*crosses*, Perseus OB1; *circles*, Cepheus OB3). The extinction of Cepheus OB3 probably occurs in clouds close to the association, while it is more truly interstellar for Perseus OB1.

To the eye there is a significant difference between the ratio of $A_{4430}/E(B-V)$ for the two associations in Figure 2. The dashed line is the best linear fit to the points for Perseus OB1 assuming values of 0.4 and 0.05 for the rms errors in A_{4430} and $E(B-V)$ respectively. The equation is

$$A_{4430} = 1.17 + 7.88E(B-V) . \quad (1)$$

The standard deviation in the residuals of the points for Perseus OB1 from the dashed line is 0.79 in units of A_{4430} when the residuals are measured perpendicular to the line. The predicted standard deviation is 0.56 from the associated rms errors. This suggests that the assumed errors are low by $\sim 20\%$, or that there is another source of variation.

The standard deviation in the residuals of the points for Cepheus OB3 from the dashed line in Figure 2 is 2.79. This treatment does not reflect the systematic nature of the effect seen by eye in Figure 2 but implies that it is significant above the 3 σ level.

In Figure 3 the dashed line is the best-fitting straight line for the Perseus OB1 points assuming rms errors of 0.05 in each color. The standard deviation in the residuals of the points for Perseus OB1 measured perpendicularly from the line in units of $E(22-33)$ is 0.30, and for Cepheus OB3 the standard deviation is 0.64. The expected standard deviation from the assumed errors is 0.33. In this case the systematic deviation for Cepheus OB3 can be considered to be at the 2 σ level. The equation for the best-fitting straight line is

$$E(22-33) = -0.32 + 5.68E(B-V) . \quad (2)$$

In Figures 4 and 5 the differences in the distributions are so well marked that we have not applied any statistical tests for significance.

Attention was first drawn to regional variations in the $A_{4430}/E(B-V)$ ratio seen in Figure 2 by Duke (1951), and later Walker (1963) found that the Perseus region had a significantly low value. It is also the region with the highest average ratio of polarization to reddening, which is the effect shown in Figure 5, and it also has the greatest degree of polarization vector alignment (Hiltner 1956). It appears to us from this analysis that there is a connection in the Per OB 1 association between the three effects of weaker A_{4430}, enhanced $E(15-18)$, and alignment of the interstellar grains responsible for polarization. If the marginally higher value of $E(22-33)/E(B-V)$ in Figure 3 is ascribed to a difference in the strength of the 2200 Å interstellar feature, then the latter would appear to be slightly strengthened in regions of strong polarization.

In Figure 6 the residuals, $(O-C)$ A_{4330}, are plotted against $E(15-18)$ for the stars in Perseus OB1 and Cepheus OB3 using equation (1) for the calculated values of A_{4330}.

Without more extensive data, particularly for polarization, from a wider range in Galactic longitude it is not clear whether the unusual results for the stars in Per OB1 reflect an actual connection between $E(15-18)$, polarization, and A_{4430} or simply independent regional variations in grain characteristics and the abundance of the 4430 Å DIB absorber. Nonetheless, the obvious correlation in Figure 6 suggests a connection between the A_{4430} residuals and $E(15-18)$.

We speculate, qualitatively, that the correlations can be explained if the 4430 Å DIB arises in a thin grain mantle and the 2200 Å feature arises in the grain core. For elongated, partially aligned grains, the effective grain diameter is reduced in viewing directions normal to the rotation axes if the latter are aligned by paramagnetic relaxation (Martin 1978). This effectively increases the number of small particles, which leads

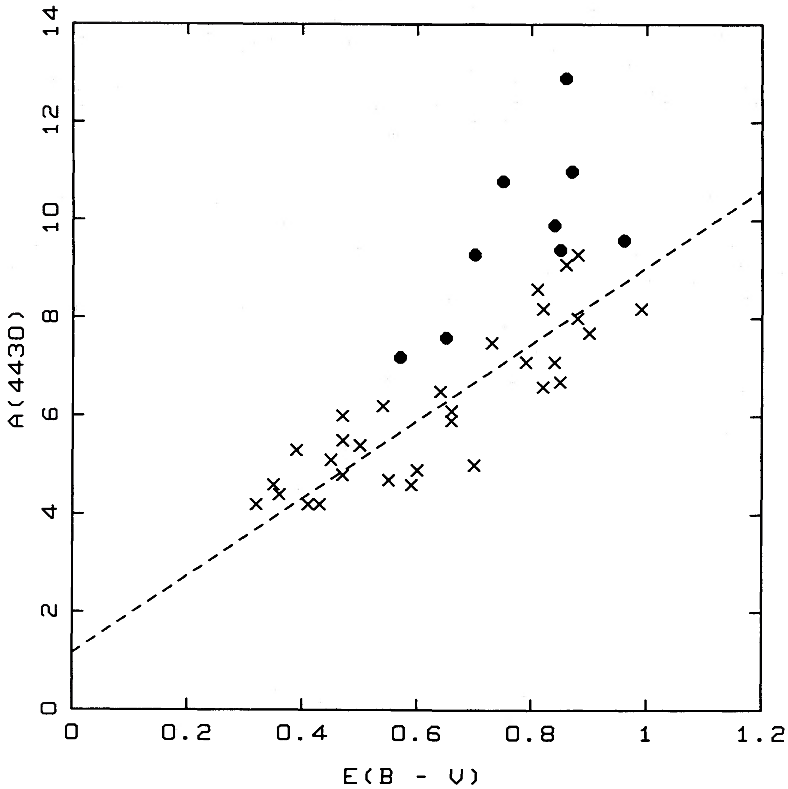

FIG. 2.—A_{4430} vs. $E(B-V)$ for the stars in Perseus OB1 (*crosses*), and Cepheus OB3 (*circles*). *Dashed line*, best-fitting straight line for the Perseus OB1 data.

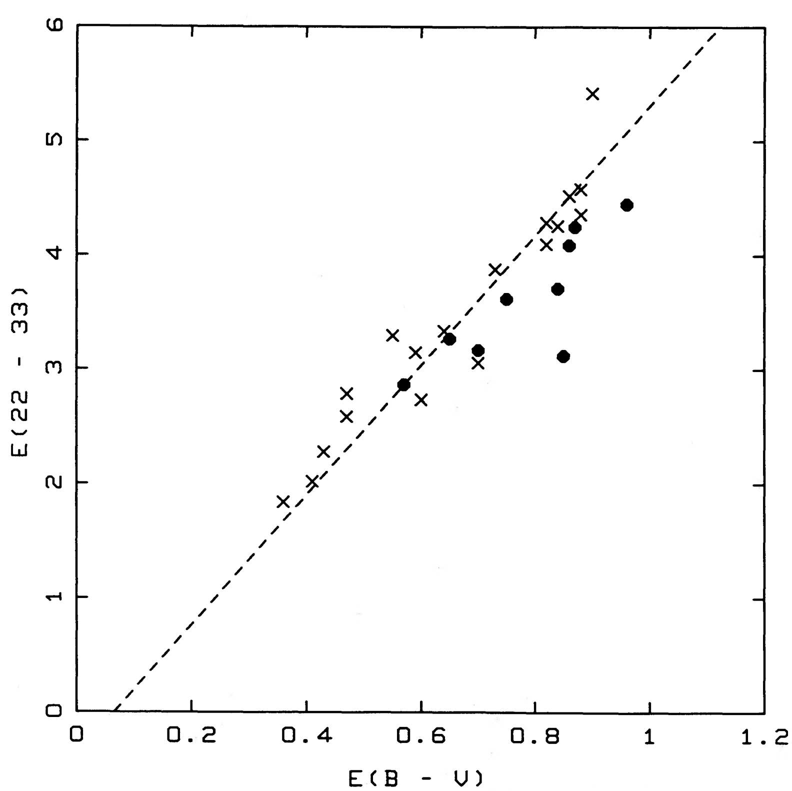

FIG. 3.—Same as Fig. 2, $E(22-33)$ vs. $E(B-V)$

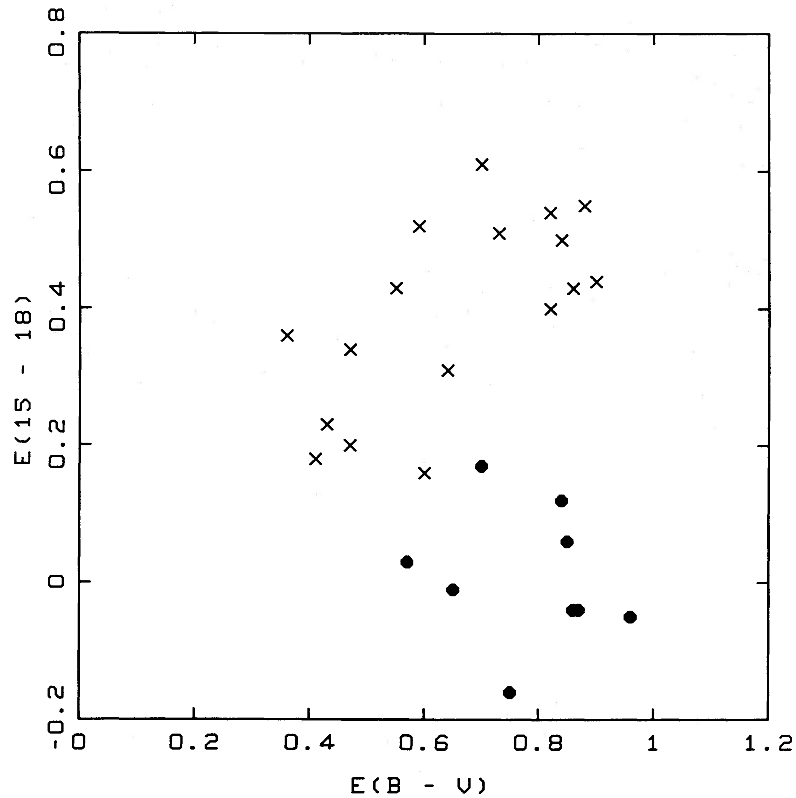

FIG. 4.—Same as Fig. 2, $E(15-18)$ vs. $E(B-V)$

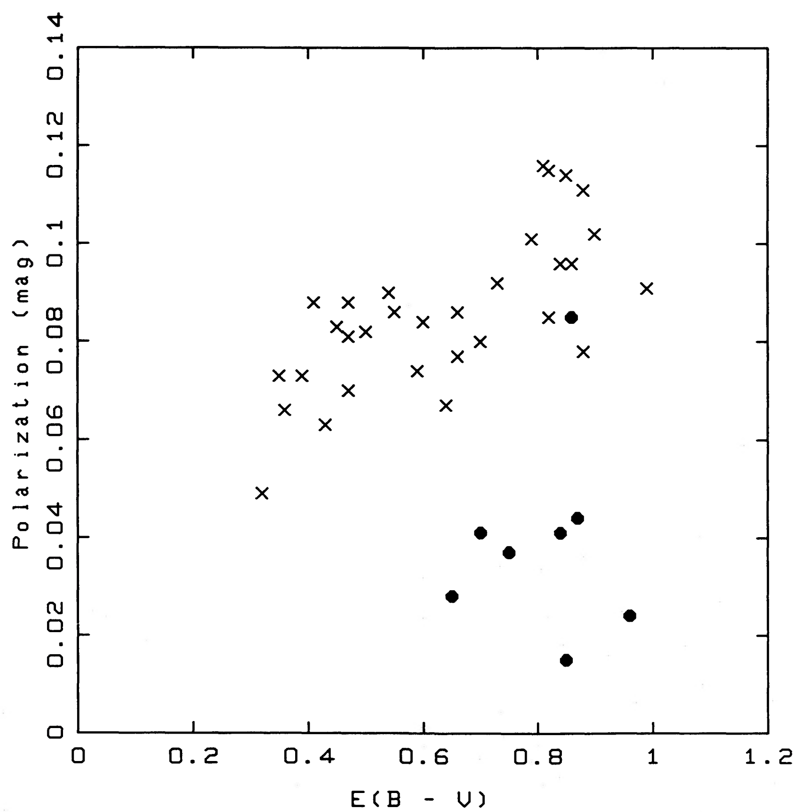

FIG. 5.—Same as Fig. 2, polarization vs. $E(B-V)$

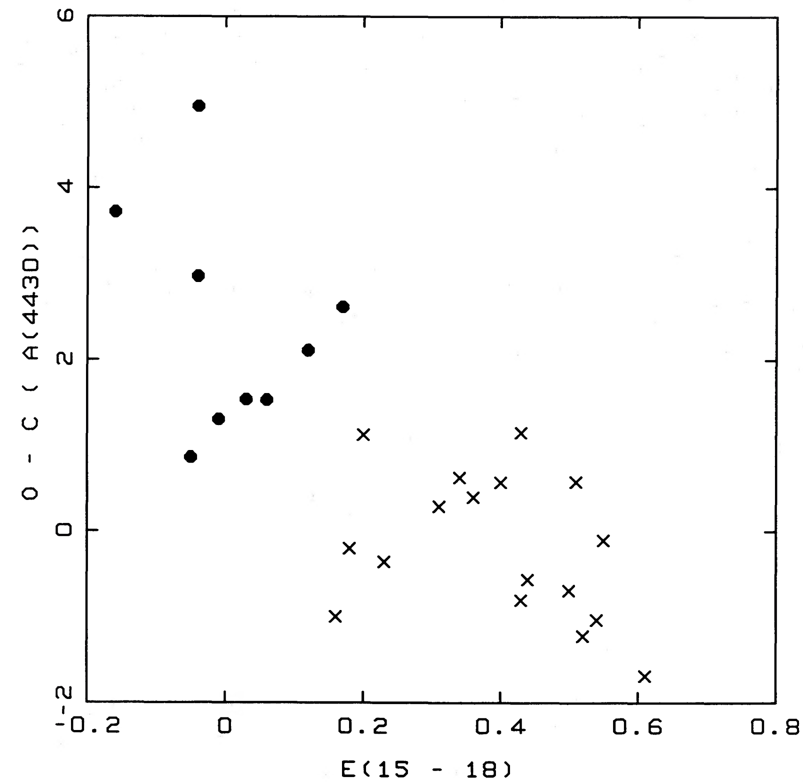

FIG. 6.—Same as Fig. 2, residuals $(O-C)$ A_{4430} vs. $E(15-18)$

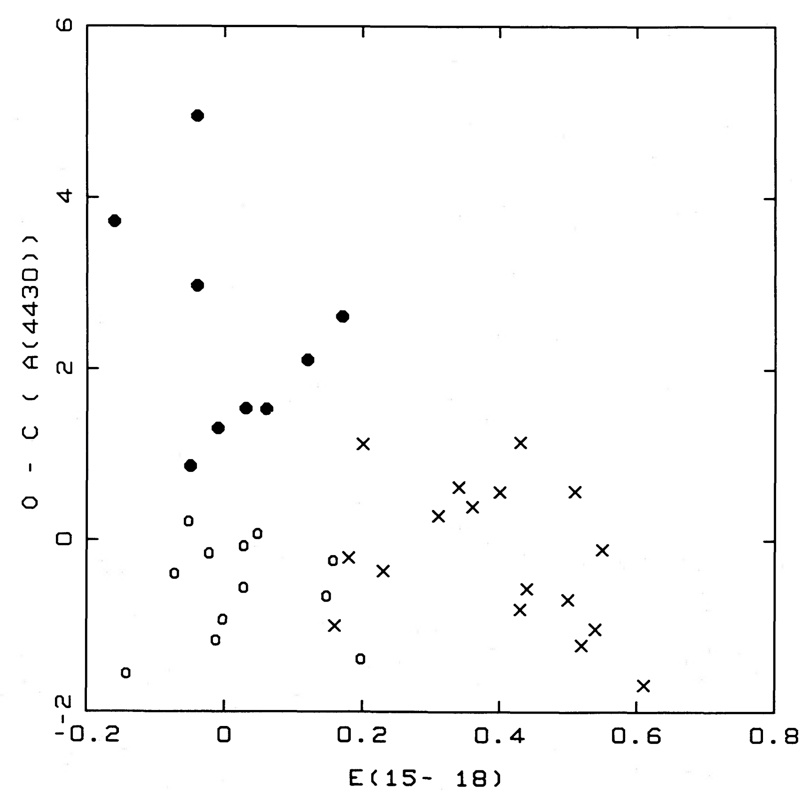

FIG. 7.—Same as Fig. 6 including stars with $b > 10°$ (*open circles*) from Table 1

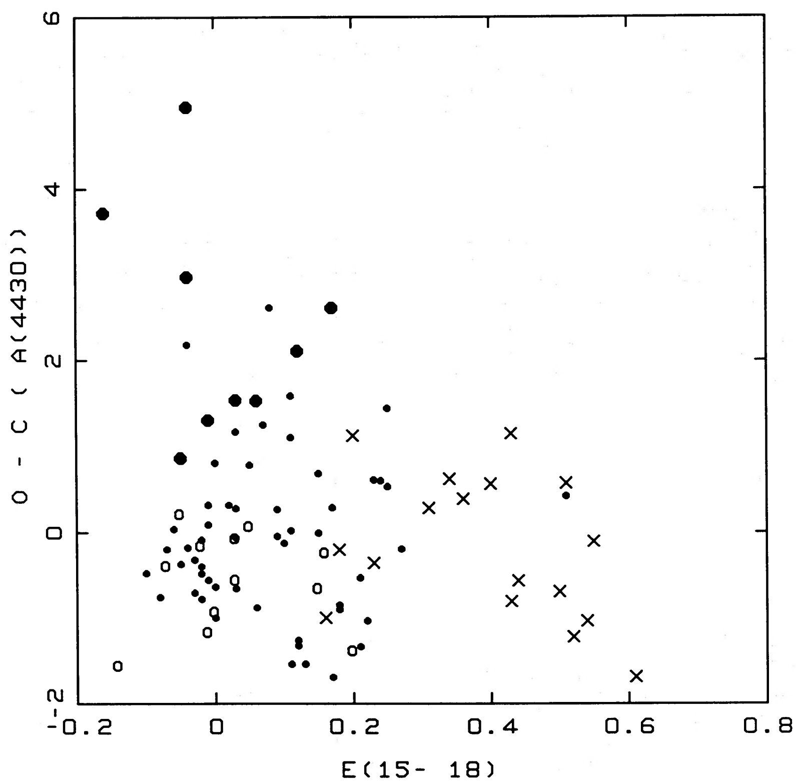

FIG. 8.—Same as Fig. 7 with all the stars from Table 1. Additional stars shown as dots.

to an enhanced ultraviolet extinction compared to a cloud in which the grain orientation is random.

If the mantle thickness is much less than 4430 Å, the ratio of the absorption to geometrical cross section at 4430 Å will be much reduced for a cylindrical grain seen end-on compared to one viewed from the side. This reduction will affect the observed strength of the 4430 Å DIB for partially aligned grains. Assuming that the core radius is greater than 2200 Å, the reverse would be true at 2200 Å.

The absence of the 4430 Å DIB in interstellar clouds at high Galactic latitudes (Krełowski and Walker 1987) would be explained by a lack of grain mantles in such clouds.

This interpretation gains some support from Figure 7, which is the same as Figure 6 with the addition of points for stars in Table 1 at Galactic latitudes above 10°. The latter populate the lower left corner of the plot. There are no polarization measurements available for most of these stars, but, assuming that the values are small, one can interpret the low values of A_{4430} as being due to thin or missing mantles in their case.

In Figure 8 values of $(O-C)$ A_{4430} are plotted against $E(15-18)$ for all the stars with such data in Table 1. (The additional stars are marked as small dots.) The distribution is triangular with the points for Cepheus OB3, Perseus OB1, and the high Galactic latitude stars defining the corners which, in our interpretation, correspond to nonaligned grains with mantles, aligned grains with mantles, and grains with thin or no mantles respectively.

If A_{4430} is affected by grain orientation, interstellar polarization within the 4430 Å band should be higher than in the nearby continuum. For stars in Per OB1 the median polarization and A_{4430} are 8% and 6% respectively. The excess of polarization expected within the 4430 Å DIB would be 0.5%. For a 3 σ detection, this requires a precision of ~0.1% of the continuum, which is feasible with current detectors if made differentially.

Additional strong support for the concept of families of DIBs is given by the ratios $A_{4430}/E(B-V)$ and 5780/5797 in Table 2. The measurements were made from Reticon spectra,

TABLE 2

THE DIB RATIOS λ5780/λ5797 AND λ4430/$E(B-V)$

HD	Sp.	l	b	$E(B-V)$	$A_c(\lambda5780)/A_c(\lambda5797)$	$A_c(\lambda4430)/E(B-V)$
2905	B1 Ia	120°8	+0°1	0.31	1.73	16.77
8065	A0 Ia	124.6	+16.1	0.38	0.92	6.58
24398	B1 Ib	162.3	−16.7	0.29	0.69	1.72
30614	O9.5 Ia	157.4	−10.1	0.29	1.06	7.24
40111	B1 Ib	184.0	+0.8	0.16	1.91	16.88
149757	O9.5 V	6.3	+23.6	0.33	0.79[a]	1.51
207260	A2 Iae	102.3	+5.9	0.45	1.29	11.78

[a] Determined by Westerlund and Krełowski 1986.

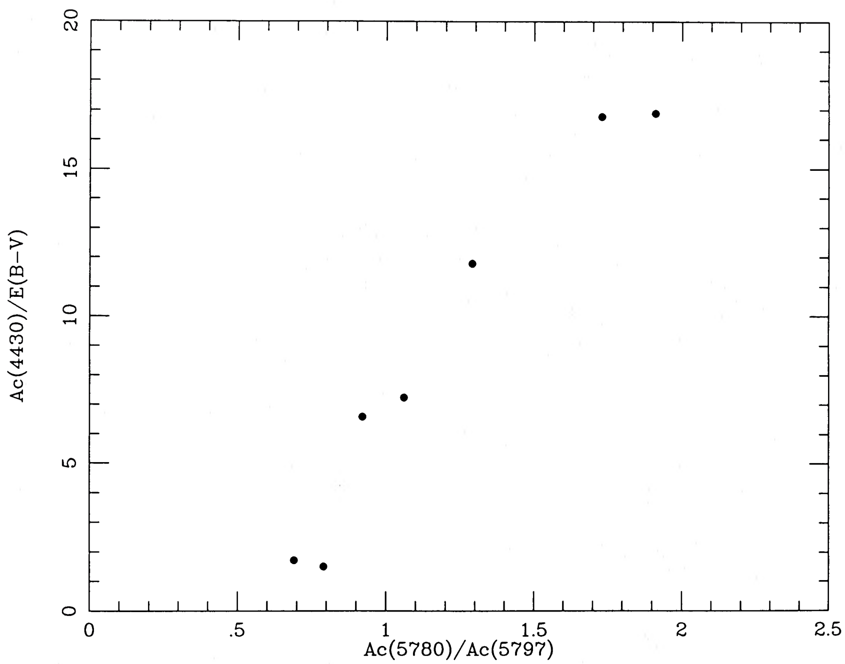

FIG. 9.—$A_{4430}/E(B-V)$ vs. DIBs ratio $\lambda5780/\lambda5797$ for the seven slightly reddened stars in Table 2 at both high and low Galactic latitude

as outlined in Krełowski and Walker (1987), and for the four stars at high Galactic latitude are taken from that paper, and new values are given for three "normal" stars of similar reddening. The ratios are plotted in Figure 9.

The three DIBs come from each of the three families, and the ratios show an extremely tight, possibly nonlinear correlation. The nonzero intercept on the $\lambda5780/\lambda5797$ axis and the positive gradient of the correlation are compatible with 4430 Å being reduced to very small values and 5780 Å to intermediate values for stars at high Galactic latitudes.

We are very grateful to Dr Stephenson Yang for assistance with the data reductions. This research was funded through grants from the Natural Sciences and Engineering Research Council of Canada to G. A. H. W.

REFERENCES

Baerentzen, J., Gammelgaard, P., Hilberg, T., Jorgensen, K. F., Kristenson, H., Nissen, P. E., and Rudkjøbing, M. 1967, *J. Obs.*, **50**, 83.
Duke, D. 1951, *Ap. J.*, **113**, 100.
Galecki, L., Graczyk, M., Janaszak, E., Kolos, R., Krełowski, J., and Strobel, A. 1983, *Astr. Ap.*, **122**, 207.
Hiltner, W. A. 1956, *Ap. J. Suppl.*, **2**, 389.
Krełowski, J., and Walker, G. A. H. 1987, *Ap. J.*, **312**, 860.
Martin, P. G. 1978, *Cosmic Dust* (Oxford: Oxford University Press).
Merrill, P. W. 1936, *Ap. J.*, **83**, 126.
Seddon, H. 1967, *Nature*, **214**, 257.
Walker, G. A. H. 1963, *M.N.R.A.S.*, **125**, 141.
Walker, G. A. H., Johnson, R., and Yang, S. 1985, *Adv. Electronic Electron Phys.*, **64A**, 213.
Wampler, E. J. 1966, *Ap. J.*, **144**, 921.
Wesselius, P. R., van Duinen, R. J., de Jonge, A. R. W., Aalders, J. W. G., Luinge, W., and Wildeman, K. J. 1982, *Astr. Ap. Suppl.*, **49**, 427.
Westerlund, B. E., and Krełowski, J. 1986, preprint.
Wilson, R. 1958, *Ap. J.*, **112**, 57.

JACEK KREŁOWSKI: Institute of Astronomy, N. Copernicus University, Chopina 12/18, P1-87-100 Toruń, Poland

G. R. GRIEVE, G. M. HILL, and G. A. H. WALKER: Geophysics and Astronomy Department, University of British Columbia, Vancouver, B.C. V6T 1W5, Canada